A New Study of the Magnetospheric Electron Environment

A.L. Vampola,* J.B. Blake,† and G.A. Paulikas‡
The Aerospace Corporation, El Segundo, Calif.

The accuracy of the standard model of the magnetospheric energetic electron environment, AE4, is examined using in situ measurements made aboard a number of low-altitude and synchronous spacecraft. The results indicate that discrepancies exist in the high-energy portion of the model, resulting in errors of up to a factor of 10 in calculated fluxes. Energy transport calculations indicate that the dose received by heavily shielded components may be as much as one-and-a-half orders of magnitude greater than would be predicted by the standard model. Methods and data for obtaining a more reliable estimate of dose are furnished.

Introduction

OCCASIONALLY, a problem that has been "solved" returns to plague the unwary because the boundary conditions of the problem are subtly changed. The case of radiation hazards to electronic circuitry is an excellent example. In the early and mid-sixties, the remnants of the Starfish nuclear test provided a hostile electron environment in the Earth's magnetosphere. The lethal effect of radiation was demonstrated vividly on several satellites in orbit at the time of the test (TRACC, Transit-4B, etc). The use of devices with low tolerance to radiation damage was avoided for those satellites which had orbital requirements that took them into the region of the Starfish electrons. However, a good model of the radiation environment was needed for both mission planning and system/subsystem design. The first major model[1] was the Aerospace Electron Model-1 (AE1) and included data from virtually all electron measuring devices that had been flown on U.S. satellites up to that time (1964). Discrepancies of up to *three* orders of magnitude occurred between data sets used in that model. Obviously, the model was quite limited in accuracy: at best to perhaps an order of magnitude in the inner radiation zone and perhaps two orders of magnitude in the outer zone. (The great variability of the fluxes in the outer zone had not been established at that time.) As better data sets became available, the electron and proton models were updated periodically. With the decay of the Starfish electron contribution, the inner-zone electron environment became quite benign (relatively few electrons at energies above 1 MeV) and of concern only to sensitive sensor systems; typical electronic components were several orders of magnitude harder than the radiation doses predicted for typical missions in space. But components and missions change. Hence, the problem has returned.

Low-Altitude Environment

Figure 1 demonstrates the problem. For a typical polar-orbiting satellite, in this case a 450-n.mi. circular orbit, the radiation dose predicted by the latest NASA electron environment,[2,3] AE4/AE5, is presented along with some typical component susceptibilities. For typical shielding thicknesses (satellite skin, box walls) of about 75 mils total, the radiation environment was unimportant as long as only bipolar and T^2L circuitry was being used. The advent of large-scale use of complementary metal-oxide semiconductor (CMOS), because of the low tolerance of CMOS to radiation, brought back the radiation damage problem. The problem, of course, extends to all devices with a low threshold for radiation damage: charge-coupled devices (CCD's), op-amps, optical couplers. etc.

The lack of margin exhibited by Fig. 1 for CMOS on a typical polar orbit required a more careful analysis of the AE4/AE5 models. The models themselves admit integration errors of factors of 4 to 6 (a fact that is usually ignored by the users of these models). The sources of the error are primarily inconsistencies between data sets and lack of data at high energies. Figure 2 demonstrates the problem. The data sets disagree among themselves by two orders of magnitude. A further problem is that the highest energy point, determined by Explorer 26, comes from an instrument that could not be calibrated with energetic electrons prior to flight.[4] Hence, the high-energy extrapolation of the model is really only a guess, although the best that could be done with the data available.

Because of the severe weight penalty of unnecessary shielding, a comparison of the AE4/5 models was made with actual data from an energetic electron spectrometer flown on the OV3-3 (1966-70a) satellite in 1966. The result is shown in

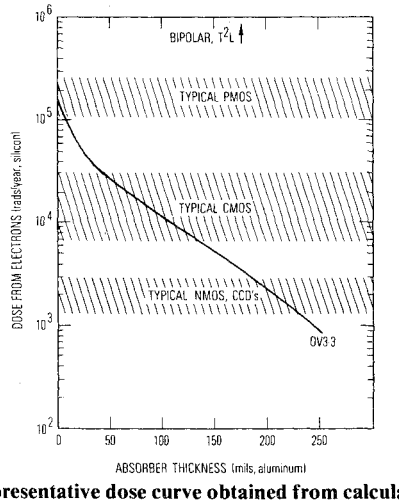

Fig. 1 Representative dose curve obtained from calculations utilizing the AE4/AE5 NASA electron environments. Cross-hatched areas represent typical susceptibility levels of various types of electron components.

Presented as Paper 77-40 at the AIAA 15th Aerospace Sciences Meeting, Los Angeles, Calif., Jan. 24-26, 1977; submitted Jan. 19, 1977; revision received July 15, 1977.

Index category: Meteoroid and Radiation Protection.

*Staff Scientist, Space Sciences Laboratory, The Ivan A. Getting Laboratories.

†Head, Particles and Fields Department, Space Sciences Laboratory, The Ivan A. Getting Laboratories.

‡Laboratory Director, Space Sciences Laboratory, The Ivan A. Getting Laboratories.

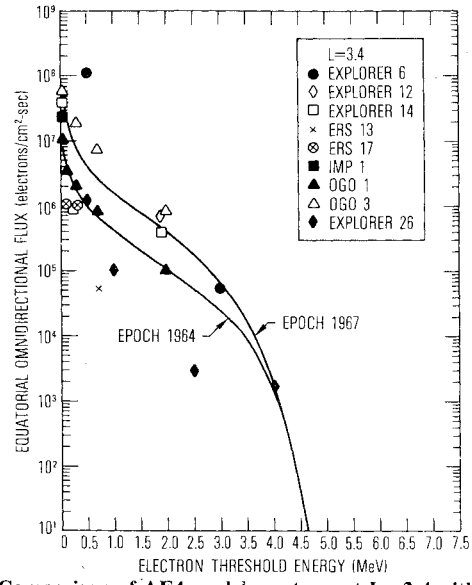

Fig. 2 Comparison of AE4 model spectrum at $L = 3.4$ with data sets used to develop the model.[2] The discrepancies probably are partially due to temporal variations.

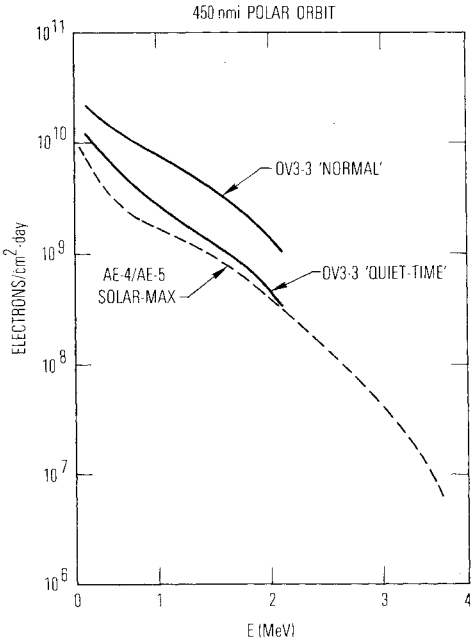

Fig. 3 Comparison of the electron spectrum in the AE4 model with the results obtained from the OV3-3 satellite for two data sets sorted according to magnetic storm history. The "average" spectrum included all data and the "quiet-time " data included only data preceded by magnetically quiet periods. All spectra are for a typical polar orbit.

Fig. 3. The agreement between the model and actual flight data in the inner radiation zone ($L \leq 2.4$, where L is McIlwain's parameter and in a dipole corresponds to the geocentric radial distance in Earth radii of the equatorial crossing of the field line) was excellent, $\leq 20\%$. However, a significant discrepancy arises when the outer-zone data are included: the model apparently is a "quiet-time" model only. Following large geomagnetic disturbances, significant fluxes of very energetic electrons appear in the outer zone and persist for some time.[5] These are not adequately modeled in the present NASA models. Since the discrepancy is in the energetic portion of the spectrum ($E > 1.5$ MeV, corresponding to a range of about 110 mils in Al), the dose effect is much larger than the fluence effect. For the 450-n.mi.

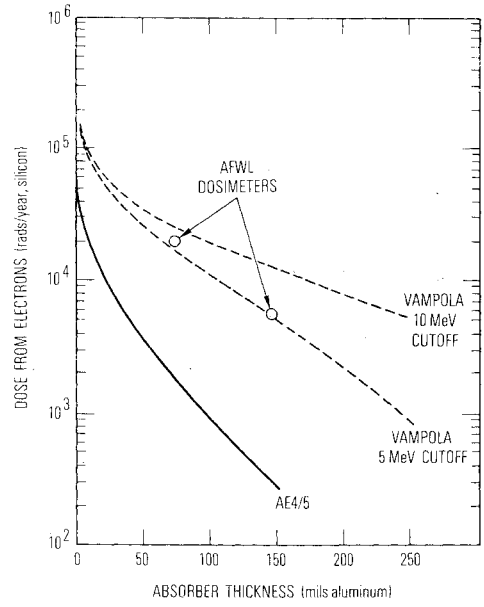

Fig. 4 Results of Monte Carlo energy transport calculations for the AE4/5 and OV3-3 "average" spectra of Fig. 3. In situ dosimeter measurements are shown for comparison.

orbit, the fluences predicted by AE4/5 and actually observed by the OV3-3 satellite differed only by a factor of 2. When calculations of dose are made, however, the difference is more like an order of magnitude for thick shields. Figure 4 demonstrates this effect. It also illustrates one of the problems common to both the NASA models and calculations using real data.

When in situ measurements of the radiation environment are made, only a portion of the spectrum is measured. In the case of the OV3-3 data set, the highest differential energy channel was 2.31 MeV. For all practical purposes, the highest reliable measurement utilized in constructing the NASA models was 1.9 MeV. Above these energies, one must extrapolate. Prior to the use of highly susceptible devices such as CMOS circuitry, the accuracy of the extrapolation was almost totally irrelevant, since the high-energy end of the spectrum contributed significant doses only to very heavily shielded components, and for typical missions that dose was orders of magnitude below the damage level.

For the purpose of calculating dose, two extrapolations of the OV3-3 data were made; one extrapolated the dose between 1.5 and 2.3 MeV to 5 MeV and assumed that the flux was zero at higher energies; the other was similar but utilized a 10-MeV cutoff. Figure 4 shows the effect of these extrapolations. Also included on Fig. 4 are two data points obtained from a composite measurement of dose made on eight different satellites utilizing approximately a dozen different dosimeters.[6] The dosimeter data covered the time period 1966-1969. The bulk of the OV3-3 results are available elsewhere.[7]

A final check of the OV3-3 results was made utilizing about 800 hr of data obtained over a period of 15 months during solar minimum on the STP72-1 (1972-76b) satellite. This satellite is in an orbit virtually identical to the 450-n.mi. orbit and should be an excellent check on the OV3-3 results (which utilized extensive extrapolations to low altitude for the 450-n.mi. result). Figure 5 shows a comparison of the STP72-1 measurements with both "quiet-time" and "average" OV3-3 data. The low-energy portion of the STP72-1 spectrum corresponds to quiet-time data (as would be expected during solar minimum), but the higher-energy portion exhibits a harder spectrum than was expected. It is probable that the effects of the August 1972 magnetic storm (one of the largest in the past two decades) on high-energy electrons in the outer

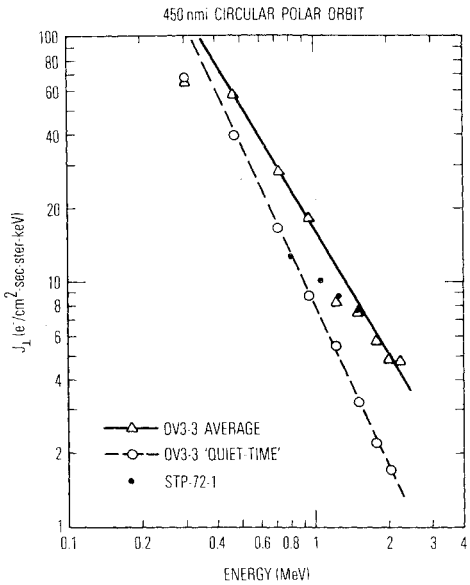

Fig. 5 Comparison of STP72-1 measurements with the OV3-3 extrapolations to the 450 n.mi. orbit.

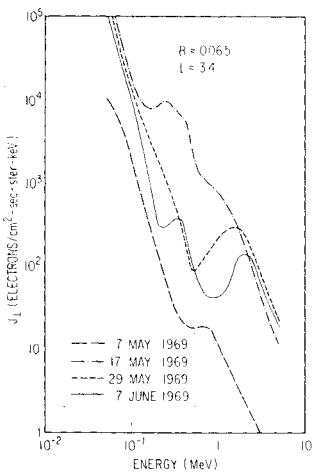

Fig. 6 Energy spectra from the OV1-19 satellite obtained preceding and following the magnetic storm on May 15, 1969.

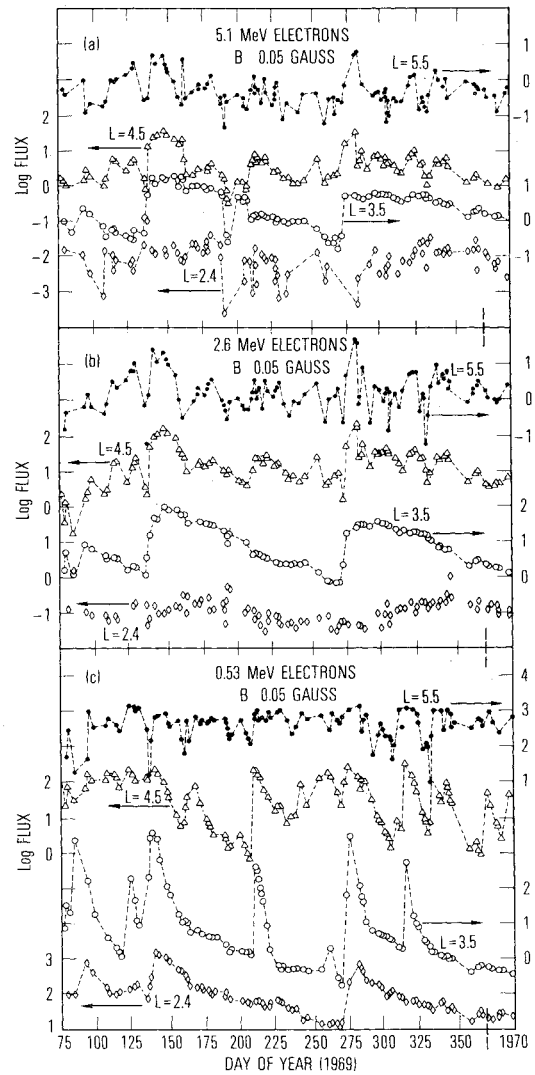

Fig. 7 Daily average fluxes at 0.53, 2.6, and 5.1 MeV at L intervals of 2.4, 3.5, 4.5, and 5.5 for the March 1969 to February 1970 period. Data are all normalized to $B = 0.05$ G. The data were obtained by magnetic electron spectrometers on the OV1-19 satellite.

zone were still present in the early data from STP72-1 (launched on Oct. 2, 1972).

Outer-Zone Electron Environment

Because the discrepancy between standard models and the actual environment appears to be limited to the outer-zone electron component, it would be useful to examine the morphology of the outer-zone electrons in detail, particularly with respect to their response to magnetic storms. Figure 6 presents a series of electron energy spectra taken just prior to, immediately after, and several weeks after the magnetic storm of May 15, 1969. The data were obtained from magnetic-focusing electron spectrometers on the OV1-19 (1969-25C) spacecraft. The instruments covered the energy range 53 keV to 5.1 MeV in 24 differential energy bands. In Fig. 6, one sees that the major effect of the storm occurs in the >200-keV range, probably because the lower-energy electrons are near some self-limiting flux most of the time. After the initial injection/acceleration, the 200-keV to 1-MeV component rapidly returns toward its initial value. However, the >2-MeV component is *still increasing* two weeks after the storm. Three weeks after the storm, the very energetic component has started to decay but is still about one-and-one half orders of magnitude greater than prior to the storm. The flux did not return to prestorm levels until several months later. To see how the outer-zone electrons respond to magnetic activity over a wide range of energy and L values, Fig. 7 was generated from the OV1-19 data. Three energy bands at four discrete L intervals are plotted from the period March 1969 to February 1970. This period should encompass the peak of the last solar cycle and should be considered representative of solar maximum.

The most dramatic effects are seen in the 0.53-MeV electron channel at $L = 3.5$. Changes of over four-and-one-half orders of magnitude are observed in response to storms. After the sharp increase, an exponential decrease is observed with a several-day time constant. Note that, although all of the storms that produce effects at $L = 3.5$ in the 0.53-MeV electrons also produce effects in the higher L intervals (further out in the magnetosphere), only two of the storms show significant effect at $L = 2.4$ (normally considered the outer edge of the inner zone in the NASA models). Also, these effects are relatively modest. The effects at higher energies at $L = 2.4$ are essentially negligible. The wide variability in the 5.1-MeV flux is due partially to the low statistics associated with counting rates near background.

At higher L intervals, even the high-energy electrons respond to relatively minor magnetic field disturbances. The 0.53-MeV electrons at $L = 5.5$ appear to be limiting at a value of flux lower than that observed in the $L = 3.5$ interval and hence do not show dramatic changes, although they do fluctuate rapidly in response to magnetospheric activity. The

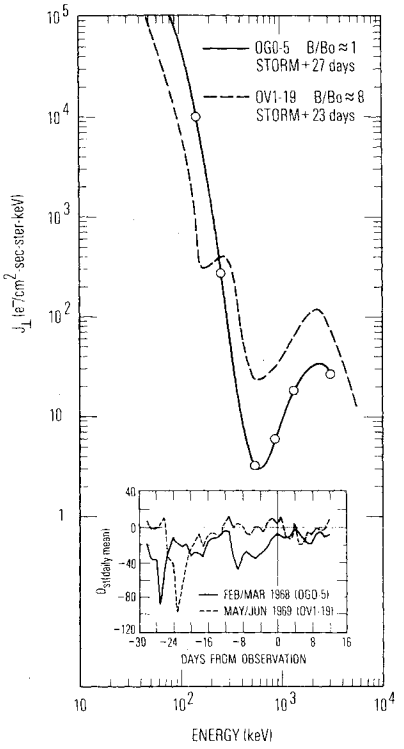

Fig. 8 Energy spectra from the OV1-19 satellite at low altitude and the OGO-5 spacecraft at high altitude for similar periods after major magnetic storms. B_0 refers to the equatorial magnetic field value. The inset details the storms in terms of D_{st}, a measure of diamagnetic effects on the Earth's field.

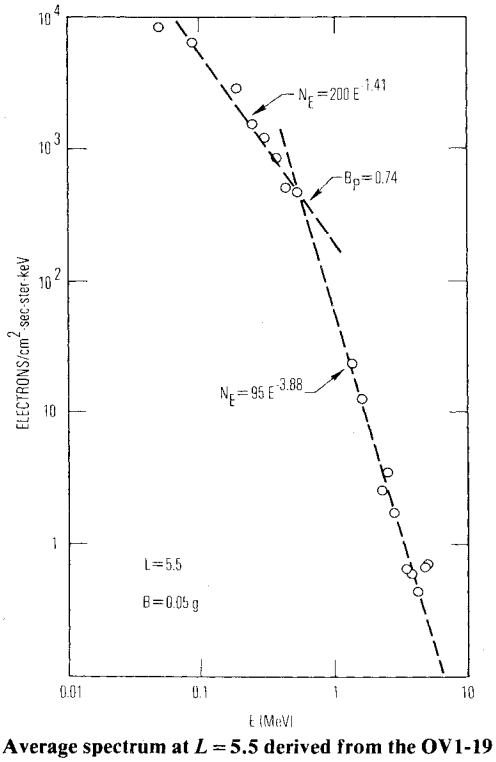

Fig. 9 Average spectrum at $L = 5.5$ derived from the OV1-19 data set showing the derivation of the coefficients given in Table 1. B_p is the breakpoint in MeV for the intersection of the spectra.

higher-enegy electrons respond to the same activity with about the same magnitude of fluctuations (higher for large storms). However, the response in the interior of the magnetosophere is different from the low-energy response. At $L = 3.5$, the 2.6- and 5.1-MeV electrons respond only to the two largest storms.

All of the data shown in Fig. 7 were obtained at altitudes between 2000 and 4500 km. (Daily averages of the measurements, appropriately normalized to $B = 0.05$ G, are shown.) With a large data base such as this extending to higher energies than have been available previously for modeling purposes, it is appropriate to attempt a refinement of the AE4/5 models. This we have done. However, first we shall show that the relatively low-altitude data from OV1-19 are representative of the environment farther up the field lines. In Fig. 8, we show data obtained from OGO-5 near the equator after a magnetic storm in 1968 (data courtesy of H.I. West Jr.). The inset in Fig. 8 shows the relationship of the OGO-5 data to the 1968 storm and the similar relationship between the data from OV1-19 at low altitude shown in Fig. 6 to its associated magnetic storm. The responses at the equator and lower on the field line show qualitative agreement. All this means is that equilibrium along the field line is achieved in a time span that is short compared to the decay time. It has been shown previously[8] that >300-keV electrons at low altitude come into equilibrium with the electrons at the equator within 0.1 days.

Having demonstrated that the low-altitude data from OV1-19 can be used for modeling the outer-zone electron fluxes, we have one further refinement to make. The data of Fig. 7 show two large storm responses. These data were obtained during solar maximum and cannot be considered to be representative of "normal" environments. Since one would expect about one major storm per year on the average, the data for the periods day 139 to 163 and day 205 to 235 were deleted from the data set. The resultant average of the data is taken to be an "average" year for the purposes of obtaining a set of coefficients for a temporary modification of AE4.

Average spectra were obtained for various L values between $L = 2.2$ and $L = 8.0$. Since we are attempting to reduce orders-of-magnitude errors in the high-energy portion of the AE4 model to factors of 2 to 4, the data points were separated into two groups that could be approximately fit with a straight line on log-log paper (i.e., functions of the form $N_E = N_0 E^{-k}$, where N is the number of electrons per cm^2-sec-sr-keV, and E is the energy of interest). Table 1 is the final result of the data reduction effort. Figure 9 demonstrates how the coefficients are defined and determined. Note that the data are normalized to $B = 0.05$ G. The actual distribution along the field line is a function of both L and magnetic local time.[9] The equatorial value may be from 6 to 20 times greater than that observed by the OV1-19 at low altitude. Hence, a reasonable assumption for high-altitude fluxes is obtained by multiplying the OV1-19 results (Table 1) by a factor of 8. This should be accurate to a factor of 2 or 3. A second approach that can be used is to merge the table spectra above 1.5 MeV to the AE4 spectra. This will produce a result that should be good to a factor of 2 or 3 (on the low side). For the purposes of calculating dose, the omnidirectional flux is required, and these values are unidirectional. A reasonable transformation from unidirectional to omnidirectional flux is to multiply the unidirectional flux by 3.5 π. This approximation should be good to about 15%. One final comment: the actual environment during a given mission can be significantly different from the averages provided by Table 1 because of the particular sequence of magnetospheric disturbances occurring during the mission. For example, a 60-day mission at 15,000 km starting at day 175 of 1969 would have seen two orders of magnitude more energetic flux (and three orders of magnitude more dose in heavily shielded components) than a similar mission starting on day 210.

Synchronous Environment

The synchronous altitude, nominally at $L = 6.6$, continues to be a region of exceptional interest because of the great number of satellite missions using and planning to use the geostationary orbit. The Aerospace experiment aboard ATS-1

Table 1 Outer-zone energy spectra coefficients[a]

L	A_1	k_1	B_p	A_2	k_2
2.2	850	-1.61	.36	4.8	-6.82
2.4	300	-2.17	.36	0.6	-8.27
2.6	41	-3.70	.40	.026	-10.8
2.8	6.4	-3.98	.42	.11	-6.29
3.0	67	-2.04	.30	30	-2.70
3.25	24	-2.42	.32	13	-2.86
3.50	105	-1.66	1.10	110	-2.58
3.75	170	-1.41	1.15	190	-2.00
4.00	160	-1.62	2.80	480	-2.66
4.25	195	-1.54	1.10	210	-2.22
4.50	235	-1.51	1.35	360	-3.08
4.75	220	-1.54	1.40	470	-3.74
5.00	235	-1.46	1.00	235	-3.58
5.25	240	-1.42	.91	190	-3.85
5.50	200	-1.43	.74	95	-3.88
5.75	120	-1.78	.75	60	-4.15
6.00	50	-2.42	1.00	50	-4.19
6.25	33.5	-2.29	.54	13.0	-3.88
6.75	9.2	-2.68	.70	3.9	-4.95
7.25	2.15	-3.28	.90	1.75	-4.93
7.75	.53	-3.85	.80	.27	-6.9
8.25	.19	-3.87	.80	.04	-12.2

[a] Note: $N_E = A_1 E^{k1}$ $(E > E_{B_p})$, $N_E = A_2 E^{k2}$ $(E > E_{B_p})$, where N is in electrons/cm^2-sec-sr-keV at $B = 0.05$ G, and E is in MeV.

(launched December 1966) provided extensive data on the energetic fluxes at synchronous altitude.[10] The Aerospace experiment aboard ATS-6 (launched May 1974) has provided data to compare with the earlier ATS-1 results. The ATS-6 experiment had a channel at 3.9 MeV, whereas the highest-energy channel on ATS-1 was 1.9 MeV; however, a direct comparison can be made at the lower energies. It should be remembered that the first ATS-1 data were acquired during 1967, near solar maximum, whereas 1974 was near solar minimum. Furthermore, the two spacecraft were not stationed at the same longitude; ATS-1 is at 150°W, whereas the ATS-6 was acquired when it was at 94°W. Thus, ATS-1 is on the magnetic equator, whereas ATS-6 was at a magnetic latitude $\approx 10°$.

The ATS data were treated as follows: for each day of data, hourly averages of the count rates were formed centered on the half hour. The probability $P(F>F_x)$ of observing an integral flux greater than F_x then was calculated for each channel of data according to the formula

$$P(F>F_x) = \frac{\text{number of samples with } F>F_x}{\text{total number of samples}}$$

In Fig. 10 is shown $P(F>F_x)$ for the three ATS-6 energetic electron channels and the corresponding probability plots obtained from the AE4 model. It can be seen that the environment at the energies under consideration shows a harder spectrum than the AE4 model predicts.

In Fig. 11, the effect of the time in the solar cycle is shown in a comparison of ATS-1 data taken in 1967 and 1974. The two ATS-1 data sets acquired at 150°W long, but separated in time by 7 yr, indicate that during solar minimum the energetic electron radiation intensity increases about a factor of 2 above that found at the same place during conditions of high geomagnetic activity characteristic of solar maximum. There is also a suggestion that the spectrum has hardened somewhat in going from 1967 to 1974.

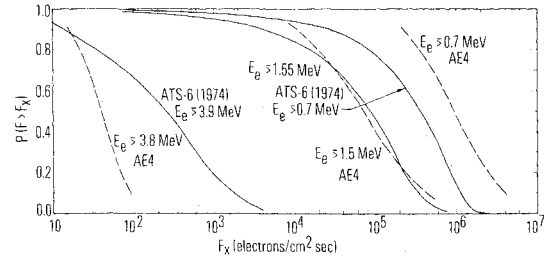

Fig. 10 Plots of the probability $P(F>F_x)$ of observing a flux of electrons greater than F_x above three integral thresholds. ATS-6 data (solid curves) and AE4 predictions (dashed curves) are shown. The ATS-6 curves were constructed using 181 days of data obtained between day 165 (1974) and day 365 (1974), while ATS-6 was located near 94°W.

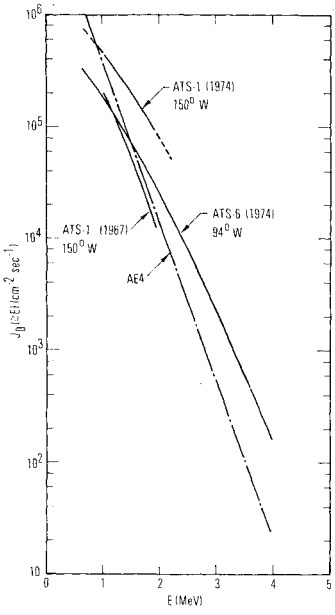

Fig. 11 Integral energy spectra constructed from the $P(F>F_x) = 0.5$ points for ATS-6 data, two sets of ATS-1 data, and the AE4 model. [Note that the $P(F>F_x) = 0.5$ point does *not* give the mean flux.]

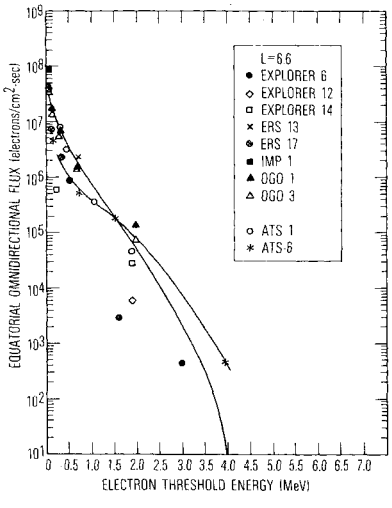

Fig. 12 Comparison of ATS-6 with the AE4 data base.

Figure 12 shows the AE4 data base for $L = 6.6\ R_e$, the AE4 model, and the ATS-6 time-averaged electron spectrum. An additional channel of ATS-6 data, covering 140-600 keV, is shown here, in addition to the three channels of ATS-6 data used in Fig. 10.

The ATS-6 data, obtained slightly off the magnetic equator, indicated fluxes about a factor of 2 lower than ATS-1 data obtained during the same time period. In other words, the 94°W location (and other similar longitudes where the magnetic equator deviates from the geographic equator) is a

more benign one. The dropoff of radiation with increasing magnetic latitude appears to be more rapid than models predict.

The ATS-6 energy spectrum is substantially harder than the AE4 model. If the ATS-6 data are normalized to AE4, at 1 MeV for example, there is about a factor of 4 higher flux for $E_e > 2$ MeV. Because the high-energy electrons dominate in the radiation dose behind thick shields, the difference between the doses calculated for the AE4 model and the ATS-6 data for parts under typical spacecraft structure is over an order of magnitude.

Conclusions

Analysis of spacecraft data have shown that the present NASA electron environment models are significantly deficient in high-energy (>1.5 MeV) electrons. Results presented here can be used to obtain a better estimate of the probable radiation dose that a spacecraft will encounter on a given mission. Ultimately, these results will be incorporated in a new NASA electron model, AE7. These results also have indicated a need for close surveillance of radiation susceptibility in new electronic technologies planned for utilization in space missions. Finally, they also have indicated a need for long-term measurement of the radiation environment in order to generate a data base from which statistically significant fluctuation parameters can be obtained for mission predictions.

Acknowledgment

Portions of the work were performed under Contracts F04701-76-C-0077 and NAS5-22450.

References

[1] Vette, J.I., "Models of the Trapped Radiation Environment Volume I Inner Zone Electrons and Protons," NASA SP-3024, 1965.

[2] Singley, G.W. and Vette, J.I., "A Model Environment for Outer Zone Electrons," National Space Science Data Center, NASA Goddard, NSSDC 72-13, 1972.

[3] Teague, M.J. and Vette, J.I., "A Model of the Trapped Electron Population for Solar Minimum," National Space Science Data Center, NASA Goddard, NSSDC 74-03, 1974.

[4] McIlwain, C.E., private communication, 1976.

[5] Vampola, A.L., "Natural Variations in the Geomagnetically Trapped Electron Population," *Proceedings of the National Symposium on Natural and Manmade Radiation in Space,* edited by E.A. Warman, NASA TM X-2440, Jan. 1972, p. 539.

[6] Janni, J., private communication, 1975.

[7] Vampola, A.L., "The Energetic Electron Environment in Circular Polar Orbits," The Aerospace Corp., El Segundo, Calif., SAMSO-TR-75-176, 1975.

[8] Williams, D.J., Arens, J.F., and Lanzerotti, L.J., "Observations of Trapped Electrons at Low and High Altitudes," *Journal of Geophysical Research,* Vol. 73, Sept. 1968, p. 5673.

[9] West, H.I. Jr., private communication, 1976.

[10] Paulikas, G.A. and Blake, J.B., "The Particle Environment at the Synchronous Altitude, Models of the Trapped Radiation Environment. Vol. III. Long Term Variations," NASA SP-3024, 1971.